4.1 CHARACTERIZATION OF ISOMERIZATION CATALYST

Isomerization catalyst is a unique recipe in terms of its key properties to be incorporated during preparation. The optimization of properties such as surface area, acidity, acid strength, crystallinity, morphology etc. are crucial for high isomerization activity. Characterization of catalysts is an important part of studies. A number of analytical techniques for the determination of physico chemical properties of the prepared catalysts. Scanning electron microscopy (SEM), X ray diffraction (XRD), Fourier transform (FTIR), Nitrogen adsorption/desorption (BET), pore volume, Temperature program desorption/Temperature program reduction (TPD/TPR) and thermal gravimetric analysis (TGA) are some important characterization tools used in this study for evaluating the physico-chemical properties of catalysts.

4.1.1 Scanning Electron Microscopy (SEM)

Scanning electron microscope (SEM) is an important and useful technique for providing the information about materials surface morphology. In this technique, when a beam of electron focuses on the sample and interact with the atoms, produces various signal, which provides the information of about sample surface and composition. Magnification and resolution are important parameter in scanning electron microscopy, which provide detailed information about sample with respect to morphology under appropriate conditions. To understand the morphology of the isomerization catalyst, the SEM images

78

were taken using [TESCAN, MIRA3, FRENCH]. Prior to testing the samples were gold coated using sputter coater, [Edward S150] to provide conductivity to the sample.

SEM images of synthesized material were shown in Fig.4.1, synthesized by hydrothermal method (ZT). The particles obtained by this method are distributed uniformly with equal grain size. It is clear from the image that the particles of zirconia are spherical with same size and are homogeneously distributed [Sagadevan et al., 2016]. At 500nm scale, it can be seen that few particles are distributed with an average size of around 30nm. SEM image of sample prepared by microwave synthesis (ZM) is shown in Fig 4.2. At 500nm range, the particles are distributed with average size of 60-70nm and they are not clearly visible. Some particles are like spherical grains and distributed homogeneously. Images of sample prepared by precipitation method (sample ID ZP) is shown in Fig 4.3. The particles are appeared to be of same grain size and homogeniously distributed with an average 30nm size. SEM images of samples prepared by sol-gel synthesis (sample ID ZG) is showen in Fig 4.4. The particles are not clearly visible and not distributed uniformly. From the image it has been observed that the particles are appeared to be around 70-80 nm size.

Fig 4.5 shows the images of sample after impregnation of TPA over the sulphated zirconia support. The morphology of impregnated sulphated zirconia is different as compared to ZP, this may be due to the presence of sulphate ions and WO3 deposited over the zirconia. The particles appeared to be different size with un-uniform distributions and particles appeared to be approximately70-80nm in size.

From the SEM images it is observed that the zirconia prepared by hydrothermal and precipitation method, consist of spherical particles uniformly distributied while in zirconia prepared by sol-gel and microwave method, particles are not uniformly distributed.
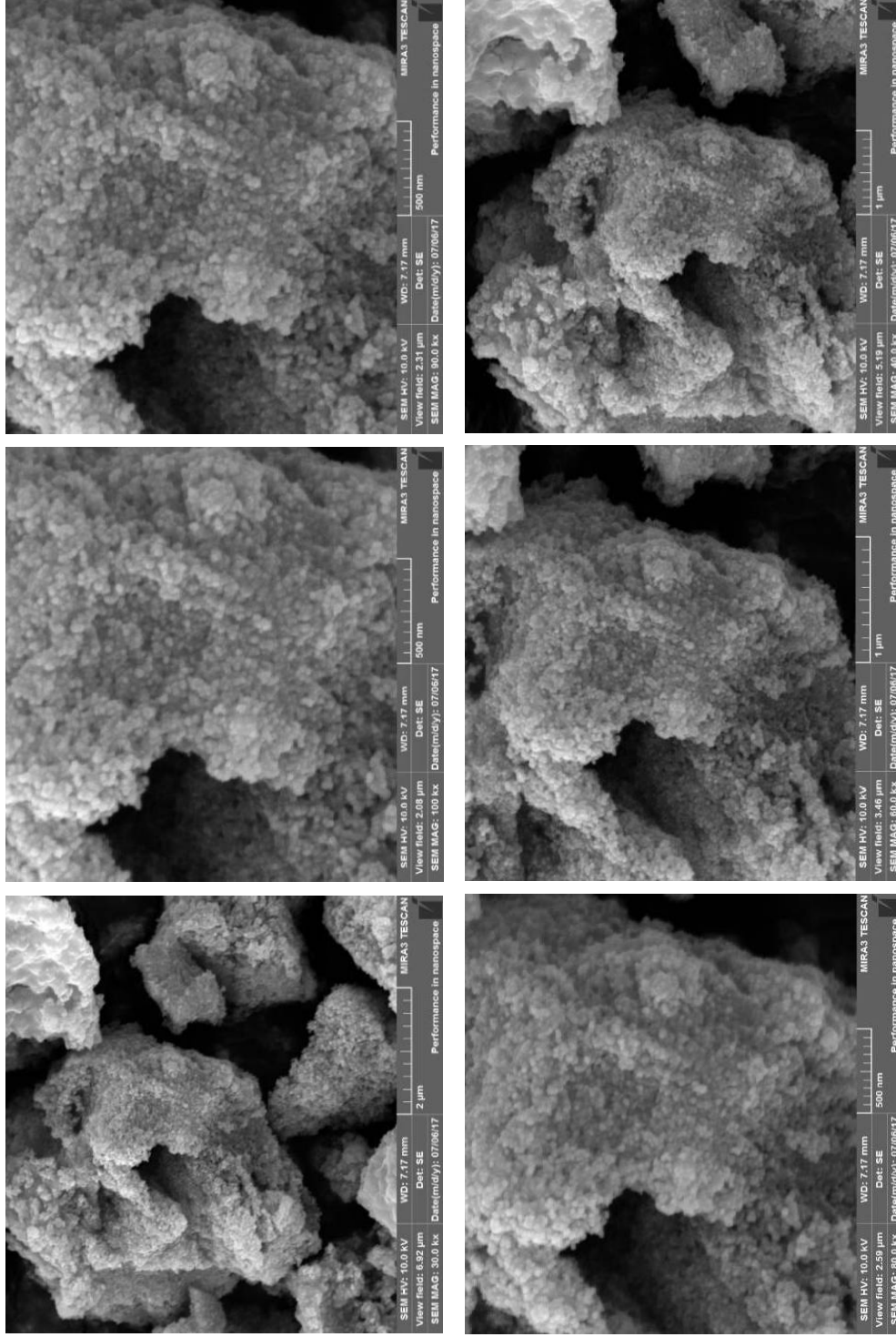
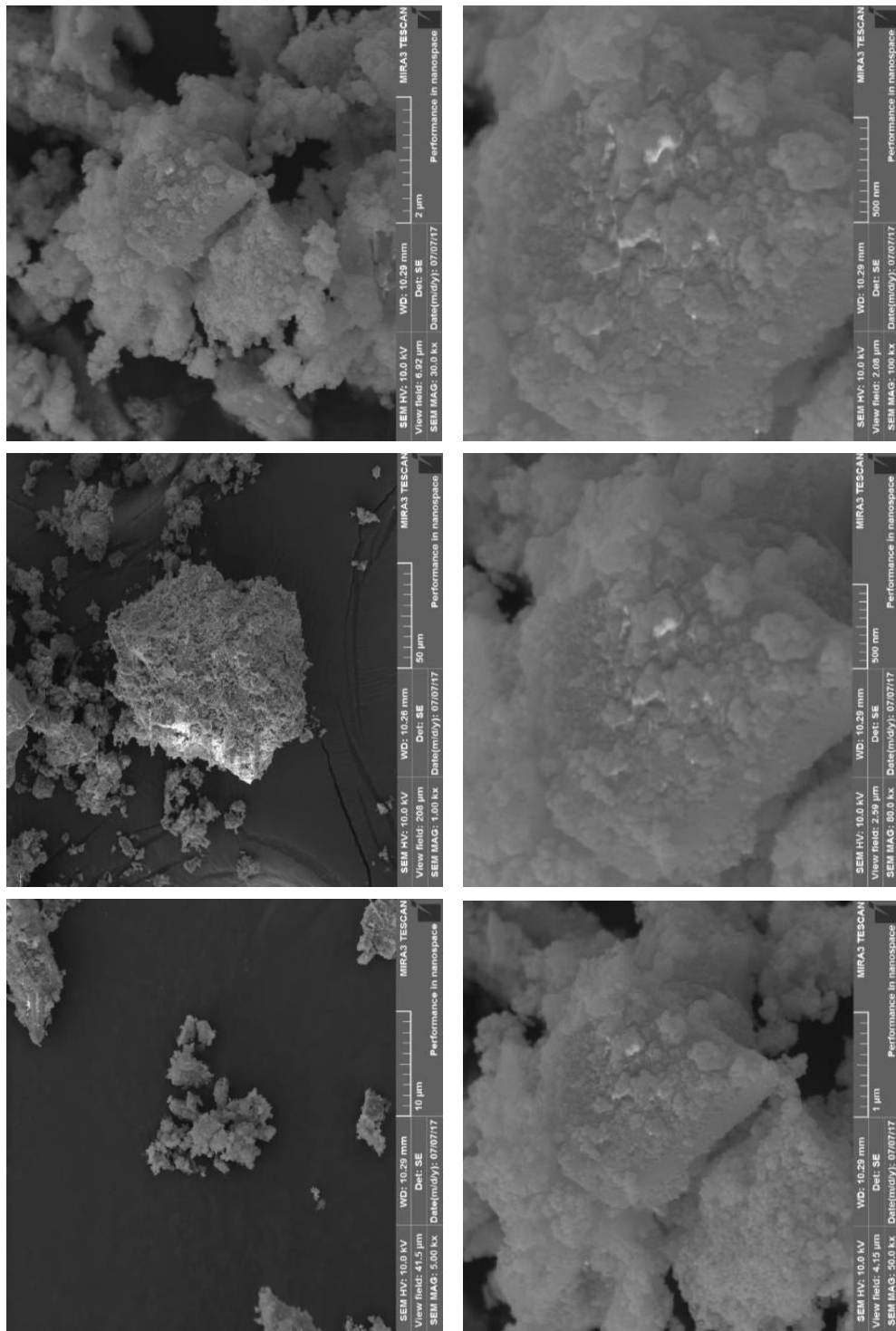**Figure 4.1 SEM Image of ZT with different magnification**
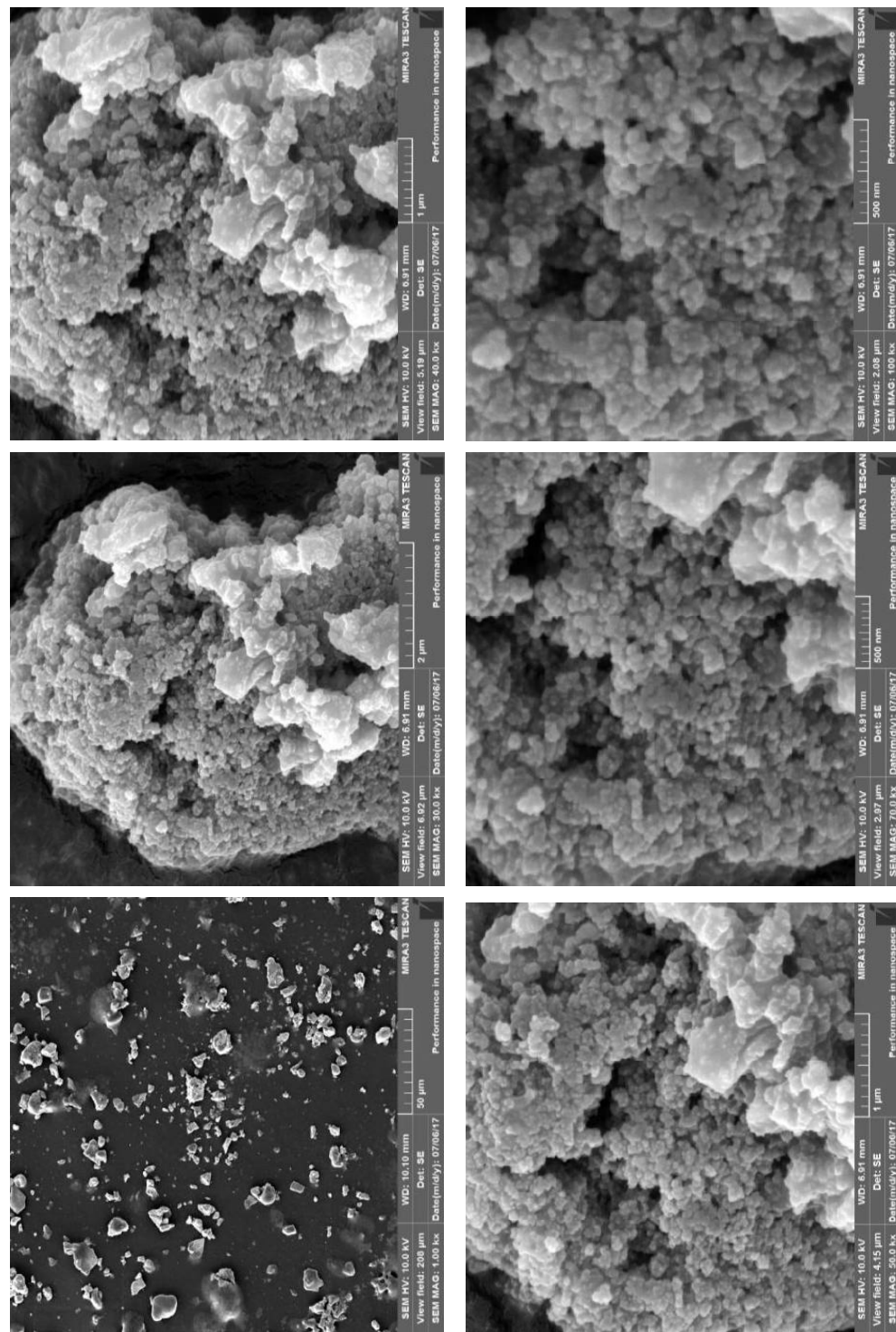
Figure 4.2 SEM Image of ZM with different magnification

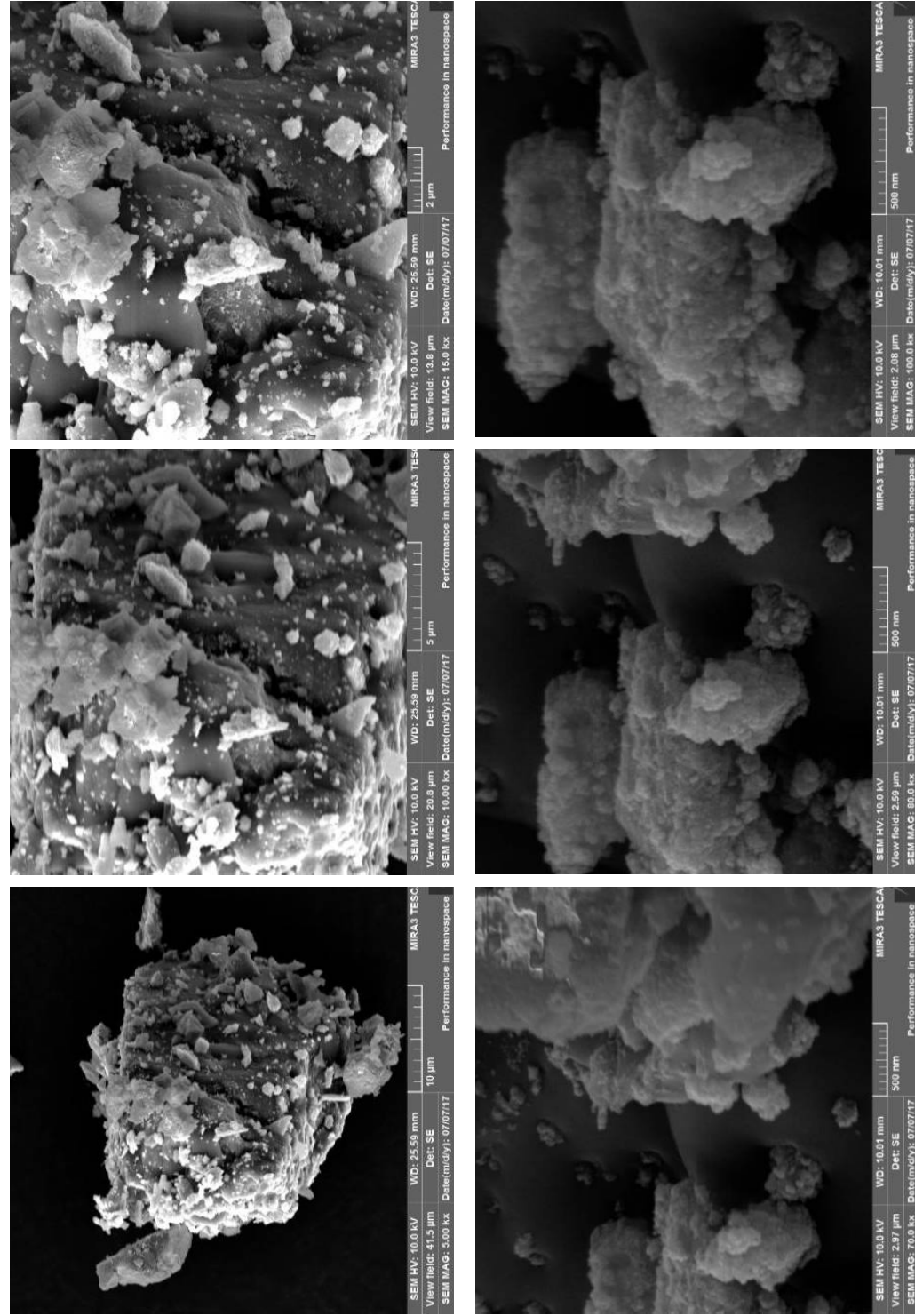81

Figure 4.3 SEM Image ZP with different magnification

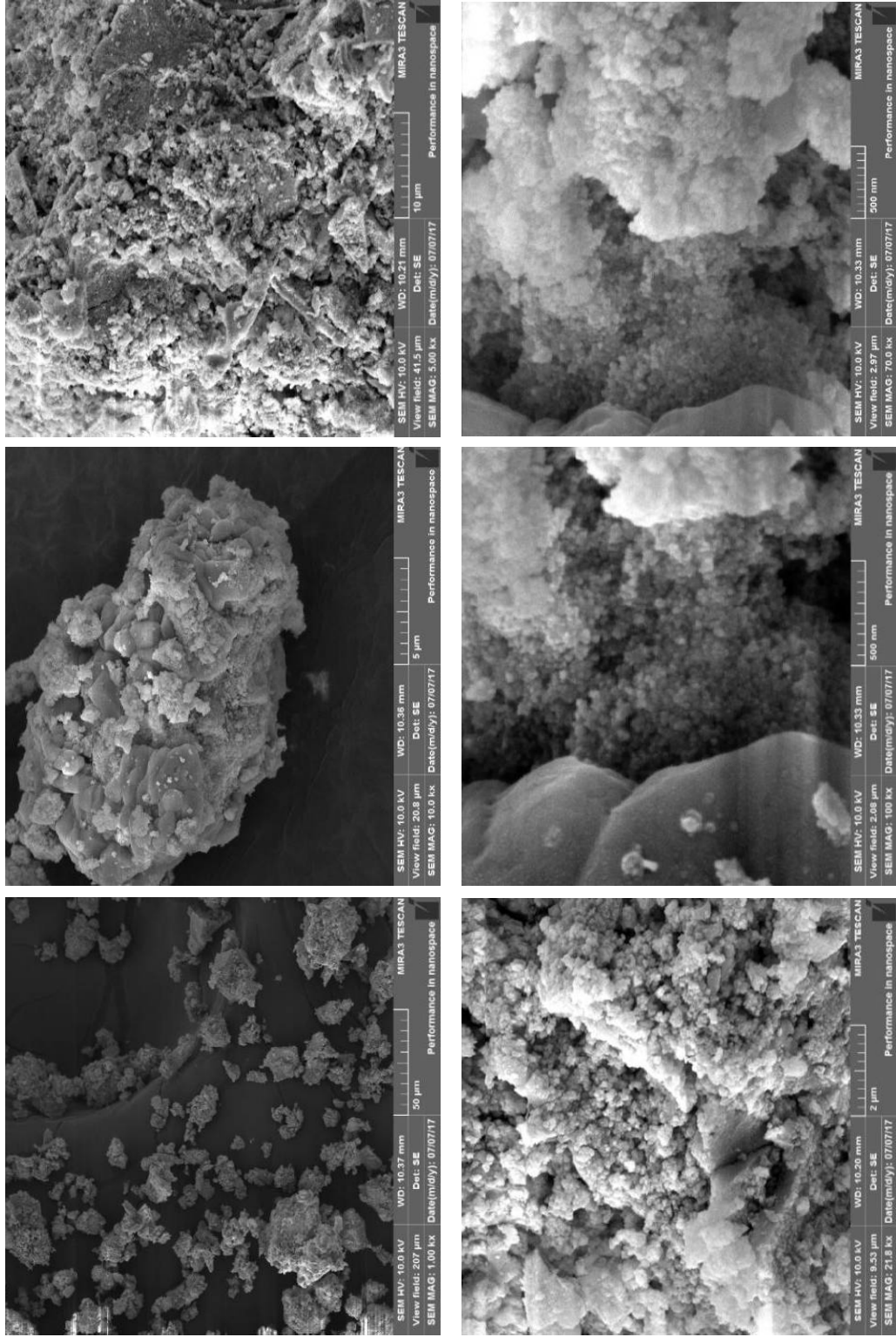**Figure 4.4 SEM Image of ZG with different magnification**

Figure 4.5 SEM Image of SZPW with different magnification

84

4.1.2 X-Ray Diffraction Analysis

X-ray powder diffraction (XRD) is an important technique for the identification of phase of materials and can deliver the information about unit cell dimensions. XRD technique is based on constructive interference of monochromatic X-rays.

The structure and phase of the catalysts were determined by X-ray diffractometer using [Bruker D8 advanced instrument, Germany] equipped with Cukα radiation with λ =1.541 Å). Operating at 40Kv volt and 30mA current. The samples were analyzed in the range 10-80° 2theta degree. The data was collected with a scan rate of $10°$ min^{-1} and with a step size of 0.2°. Sample preparation for the X-ray analysis involved grinding of the solid into a fine powder and packing of approximately 0.5gm of the sample with light compression to make it flat and tight [Mishra et al., 2002; Pichardo et al., 2008; Jentoft et al., 2004].

XRD pattern of all the synthesized zirconia samples calcined at 600°C exists in crystalline phase as shown in Fig 4.6 and Fig 4.7, while uncalcined samples exists in amorphous phase as shown in Fig 4.8. All the samples showed peaks at around $2\theta =$ 30.13°, 35.36°, 50.40°, 60.2°,62.83° and 74.5° for the tetragonal phase of zirconia, corresponding to (101), (110), (112), (200), (211), (202) and (220) planes respectively (JCPDS 80-2155) [Enriquez et al., 2012; Heshmatpour et al., 2012]. Some additional peaks were also observed at $2\theta = $ 24.50°, 28.36° 31.4°, 34.3°, 41.55°,45.59°, 54.10°, 55.54° and 65.75°, attributed to the monoclinic phase of zirconia, corresponding to (011), (111), (111), (002), (211), (202), (013) and (132) planes respectively [JCPDS card number 7-3430][Chintaparty et al., 2017; Chintaparty et al., 2016b; Enriqued et

al., 2012]. Incorporation of sulphate ions and TPA does not show any additional peaks in XRD patterns (Fig 4.2c). Some researchers have reported that the tetragonal phase of zirconia is the active phase for isomerization reaction [Torres Garcia et al., 2001]. The obtained results indicate that both the tetragonal and monoclinic phases coexists in the material. Therefore, it can be assumed that the sulphated zirconia catalyst is favorable for isomerization reaction.

The crystallite sizes (D) of the materials was calculated using the Scherrer equation (1).

$$D = \frac{0.9\lambda}{\beta \cos \theta} \qquad (1)$$

Where λ is the wavelength of radiation used ($\lambda = 1.5406$ Å), θ is the Bragg angle and β is full width at half-maximum intensity (FWHM). The presence of wide peaks could imply the existence of small crystalline particles, but not less than 5nm [Ibragimova et al., 2013]. These small particles responsible for high surface area of the catalysts. The surface impregnated sulphate ions, enhanced the surface area and effectively participate in the reaction. The average crystallite size of the samples were calculated from scherer equation was found to be approximately 26 nm, 30nm, 25nm and 31nm for ZT, ZM, ZP and ZG respectively.
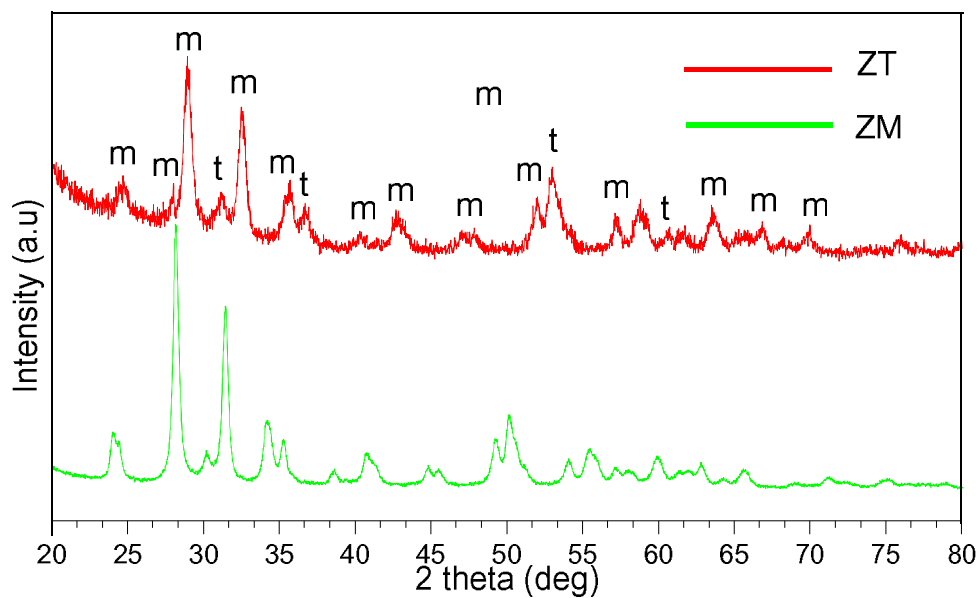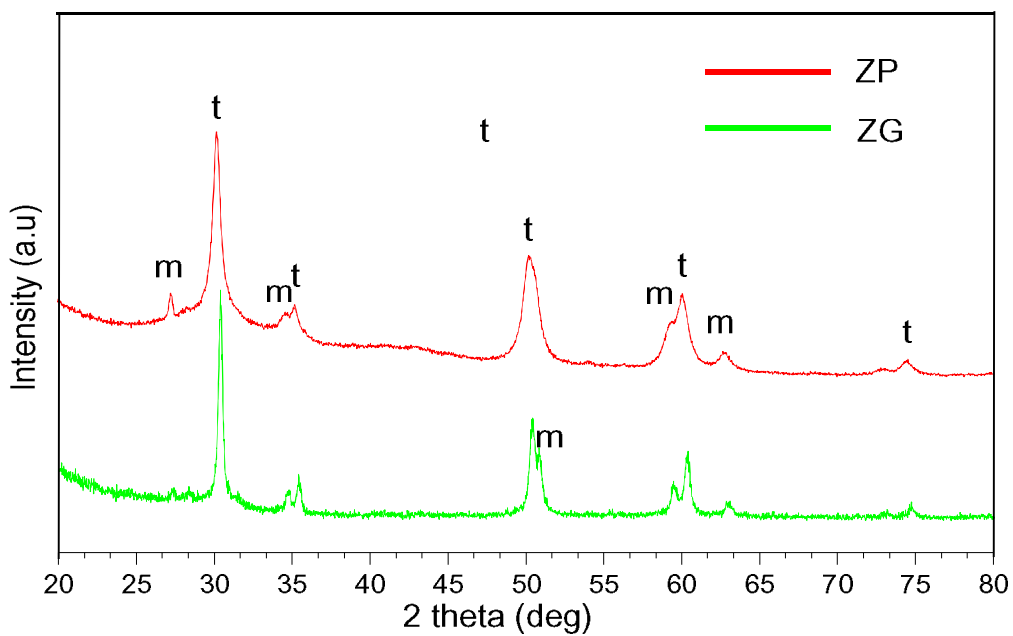
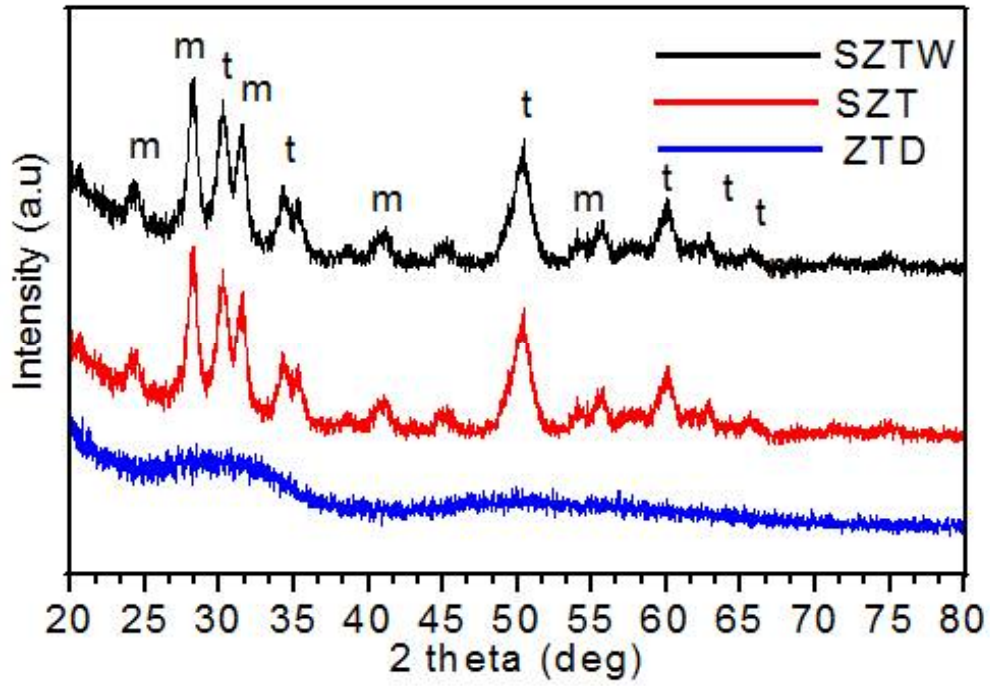**Figure 4.6**

Figure 4.7 XRD Pattern of ZP; ZG

Figure 4. 8 XRD Pattern of ZD; SZT; SZTW

Figure 4.9 XRD Instrument

4.1.3 Fourier Transform Infrared Spectroscopy (FTIR)

Fourier transform infrared spectroscopy (FTIR) [Griffiths et al., 2007] is an important technique and used for solids, liquids and gaseous samples for obtaining the information about absorption or emission of infrared radiation. FTIR deals with qualitative examination of inorganic and organic materials. It detects presence of chemical bonds in a molecule by through an infrared absorption spectrum. The spectra of the materials provide a distinctive molecular fingerprint that can be used to detect the different components present in the samples. It is an effective analytical instrument for identifying functional groups and getting information about covalent bonding.

FTIR was recorded on a [Perkin Elmer LR 64912C Fig. 13], to examine the linkages between heterometal oxide networks. The powder samples were mixed with KBr to form pellets and spectra of the prepared pellets were recorded in the frequency range of 400-4000 cm^{-1}. The FTIR spectra of pure zirconia (Fig. 4.10 and 4.11), sulphated zirconia and TPA impregnated sulphated zirconia catalyst were recorded as shown in Fig 4.12. In the FTIR spectrum of pure ZrO_2, the small bands near at 423–670 cm^{-1} corresponds to Zr-O bond, which confirms the formation of ZrO_2 structure [Sarkar et al., 2006; Singh et al., 2014]. A broad band at 3345 cm^{-1} is related to physisorbed water, whereas the band at 1633 cm^{-1} can be referred to the bending mode (H-O-H) of coordinated water [Gowri et al., 2014]. Band at 1362 cm^{-1} is attributed to the bending vibration of Zr-OH [Sinhamahapatra et al., 2011; Nakamato et al., 2008]. In the spectrum of sulphated zirconia, the bands at 980, 1071, 1174 and 1236 cm^{-1} are characteristic of asymmetric and symmetric stretching modes of oxygen bound to the sulphur of sulphate [Dou et al.2012, Radwan et al 2009; Bieletzki et al., 2010]. The

89

wave number of this band increases with the sulphur content, due to change in the type of sulphate species from isolated to polynuclear [Vishwanathan et al., 2008]. Bronsted acid sites found in sulphated zirconia samples is due to the ionic nature of S-O bond [Tran et al., 1998]. The broad band at around 3200 cm^{-1} is attributed to the O-H stretching vibration of water associated with ZrO_2 [Mishra et al., 2004]. Further, the bands in between 800-1100 cm^{-1} shown in the spectrum of material impregnated with tungstophosphoric acid reveals the presence of heteropoly acid in keggin structure. Peaks at around 1048, 890, 800, 986cm^{-1} indicates the stretching modes of oxygen atoms bonded to tungsten and phosphorus, i.e. (P-O), (W-O-W), (W=O) respectively [Yori et al., 2005, Misono et al., 1987; Sakthivel et al., 2008; Rao et al., 2008].
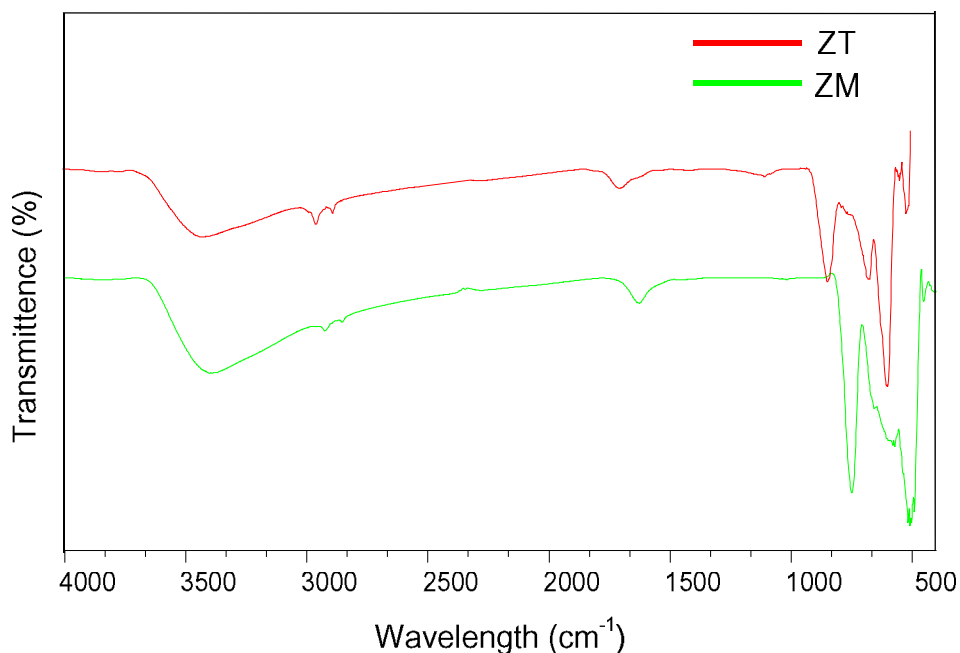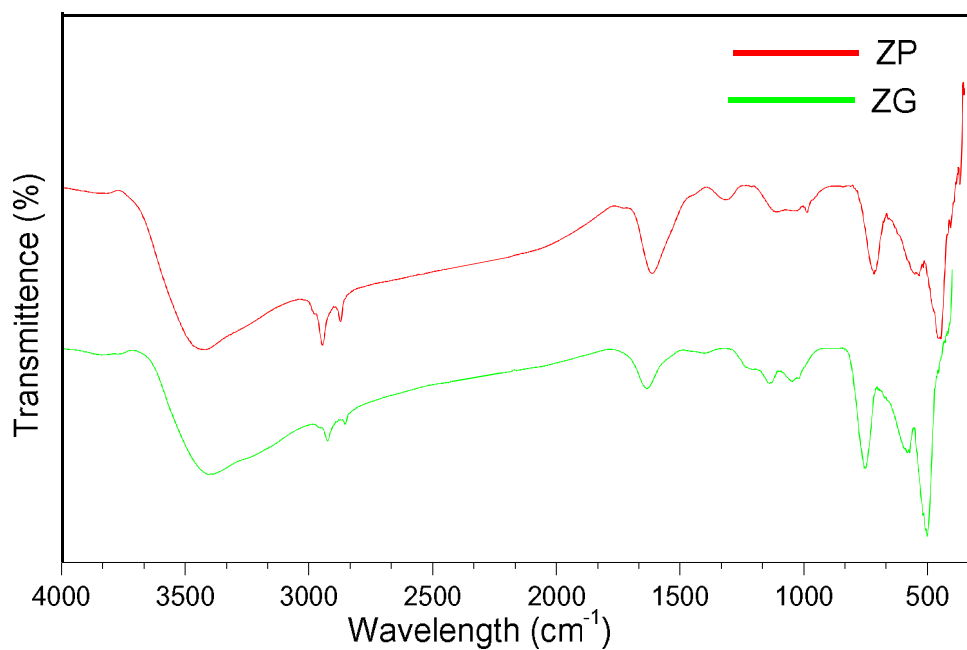

Figure 4.10 FT-IR Pattern of ZT; ZM
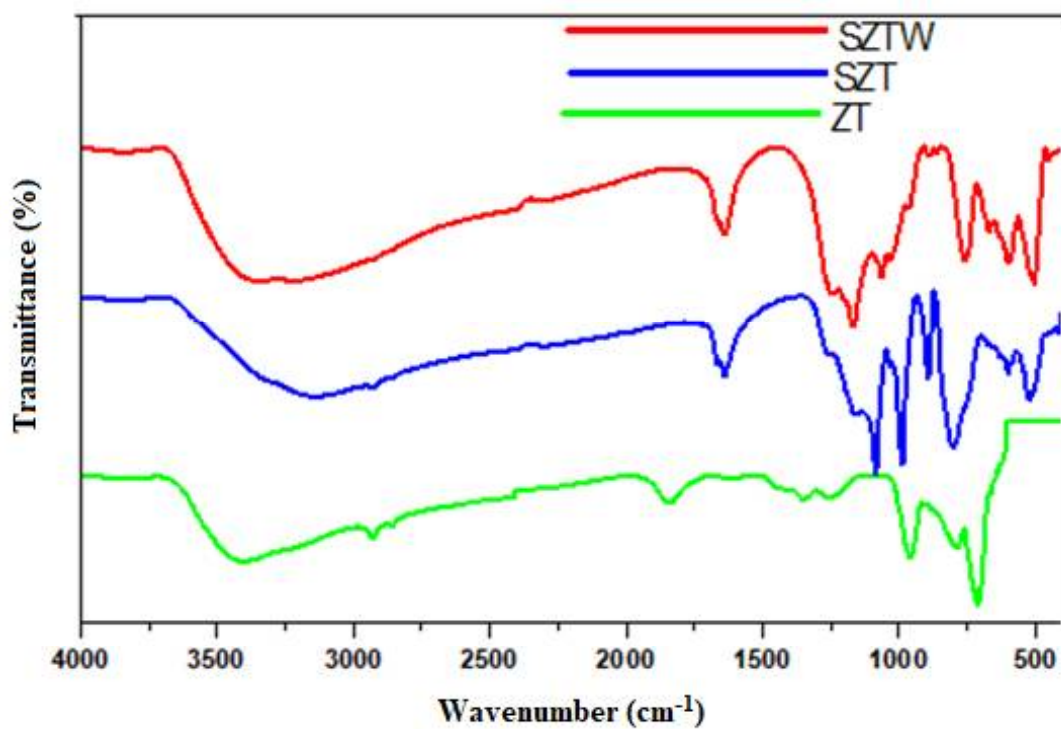
Figure 4.11 FT-IR Pattern of ZP; ZG

Figure 4.12 Pattern of   samples ZT; SZT; SZTW

Figure 4.13 FT-IR Instrument

4.1.4 N₂ Adsorption/Desorption Isotherm Analysis (BET Analysis)

Surface area of catalysts is an important parameter in the field of catalysis in governing its activity. Mesoporous silica and layered clay minerals (porous inorganic materials) have high surface area which can be calculated by the Brunauer-Emmett-Teller (BET) method. The surface area of materials is calculated by monomolecular layer adsorption of a gas on the solid surface. Physical adsorption of N_2 gas is bonded by van der Waals forces between the adsorbent surface area of the materials and the adsorbate gas molecules. The BET theory applies to systems of multilayer adsorption, and usually utilizes gases, that do not chemically react with material surfaces as adsorbates to measure specific surface area. BET value obtained by equation (1) is plotted against

P/P$_0$. Regression coefficient of straight line in the relative pressure range of 0.05 to 0.3, should not less than 0.9975.

$$\frac{1}{\left[V_a\left(\frac{P_0}{P}-1\right)\right]} = \frac{C-1}{V_m C} \times \frac{P}{P_0} + \frac{1}{V_m C}$$

.... (1)

Where,

P = partial vapor pressure of adsorbate gas in equilibrium with the surface at 77 K (b.p. of liquid nitrogen), in pascals,

P$_o$ = saturated pressure of adsorbate gas, in pascals,

V$_a$ = volume of gas adsorbed at standard temperature and pressure (STP) [273.15 K and atmospheric pressure (1.013 × 105 Pa)], in milliliters,

V$_m$ = volume of gas adsorbed at STP to produce an apparent monolayer on the sample surface, in milliliters,

C = dimensionless constant that is related to the enthalpy of adsorption of the adsorbate gas on the powder sample.

The BET surface area, pore volumes, pore size distributions, pore diameter and average particle size was measured by BET method and N$_2$ adsorption/desorption isotherm at liquid nitrogen temperature using Accelerated Surface Area and Porosimetry System [Micromeritics, ASAP 2020] Fig 4.18. All the samples were degassed at 250ºC prior to actual measurement. N$_2$ adsorption/desorption isotherms for materials is shown Fig

4.14 and Fig. 4.16. Type IV isotherms with well-defined hysteresis loops (H_3 Type) were obtained for all the prepared samples. The occurrence of conspicuous hysteresis loops at high relative pressures indicates the presence of mesoporous, non-rigid aggregates of plate-like particles (slit-shaped pores) being related to weak interaction and capillary condensation associated with large pore channels [Gregg et al., 1982; Rodrigo et al., 2015]. Among the synthesized oxides, it has been observed that the relative pressure point, where adsorption and desorption branches coincide, is affected by the type of the metal oxide present and it was found to have hysteresis at highest relative pressure. In the isotherm plot (Fig. 4.14), between P/P_0 of 0.450 and 0.970, the adsorption gradually increases uniformly. This indicates that the catalyst has uniform surface. It means that the nature of the surface is almost same throughout the catalyst and indirectly favors the isomerization as it is a surface phenomenon and the hysteresis loop generally represent the large mesoporous. In corporation of sulphate ion result in high surface area and high stability of catalyst [Yori et al., 2000]. It has been suggested by Wang and coworker in 2007 that, when H_2SO_4 has been used for the preparation of catalyst, the SO_4^{2-} ions present in the zirconia framework would replace of OH^- ions. Because, the thermal stability of the sulphate ions in the zirconium linkages is higher than hydroxyl group across two Zr atoms. For the removal of SO_4^{2-} ions these requires a higher temperature than hydroxyl ions and stabilizes the tetragonal phase at low temperature [Wang et al., 2007]. The isotherm with desorption hysteresis indicates the presence of mesoporous materials [Patra et al., 2011; Zheng et al., 2001]. Appreciable pore volume (0.27 to $0.50 cm^3 g^{-1}$) and pore diameter (6.60 nm to 7.90 nm) permit the transport of reactive molecules inside and products outside. The pore size also allowed

a free computable transport through the interior of the pores of the n-hexane molecule 8.6 [Rodrigo et al., 2015]. The pore size distributions (PSD) of the catalyst samples, measured by Non Local Density Functional Theory (NLDFT) method (using N_2 adsorption/desorption) and the corresponding plot is shown in Fig.4.15 and Fig 4.17. In addition, the volume of these pores is perfect to adsorb the alkane molecules effectively making the isomerization more facile. PSD of the final product indicates that sulphated zirconia have narrow pore size distribution as compare to pure zirconia. The intercalation of oxides and reduction of particle size to nano range could help in achieving high surface area (135 to $245 m^2 g^{-1}$). So it can be concluded, that impregnation of sulphate ions enhances the surface area of the catalysts (175 to 288 $m^2 g^{-1}$). It was also observed that the impregnation of TPA reduced the surface area (93 to 165 $m^2 g^{-1}$) and this greater surface area is one of the reasons behind the more catalytic activity. The physico- chemical properties of all catalyst is shown in Table 4.1- 4.4.
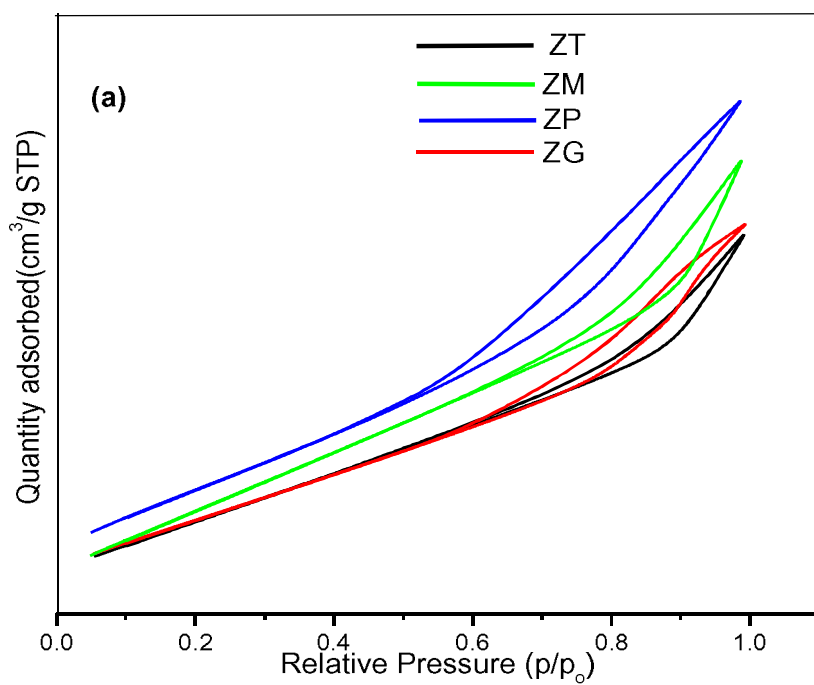
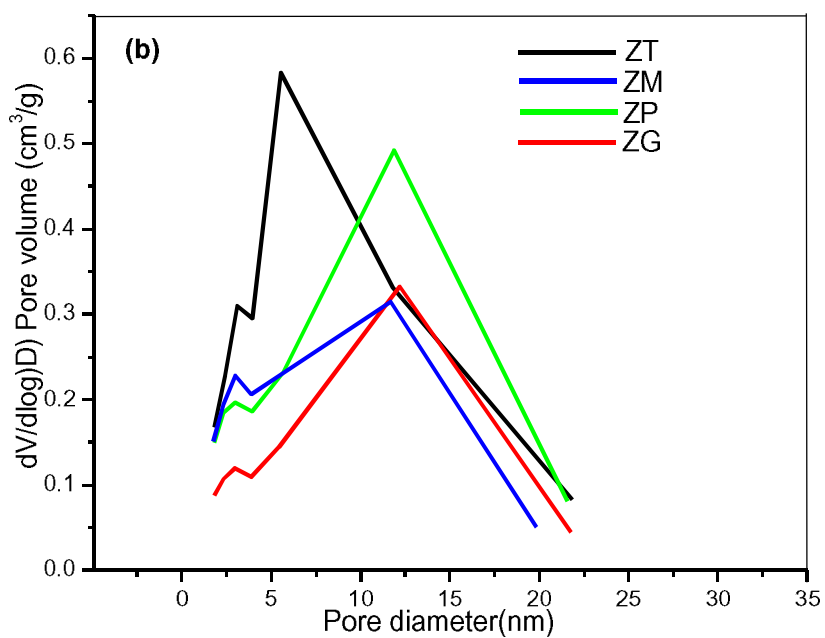**Figure 4. 14 BET Isotherm of Samples ZT; ZM; ZP; ZG**

Figure 4. 15 Pore size distribution
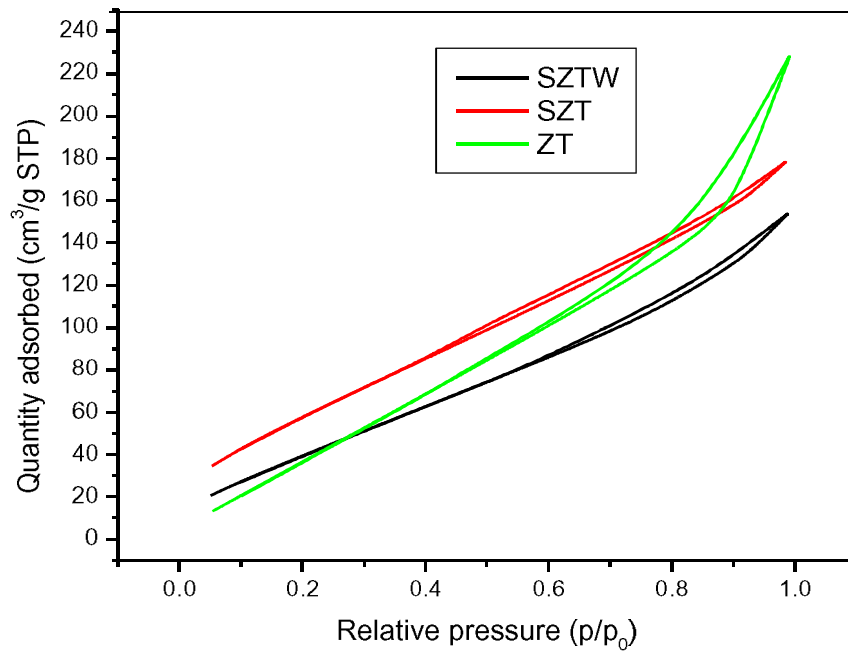
Figure 4. 16 BET Isotherm of Samples ZT; SZT; SZTW
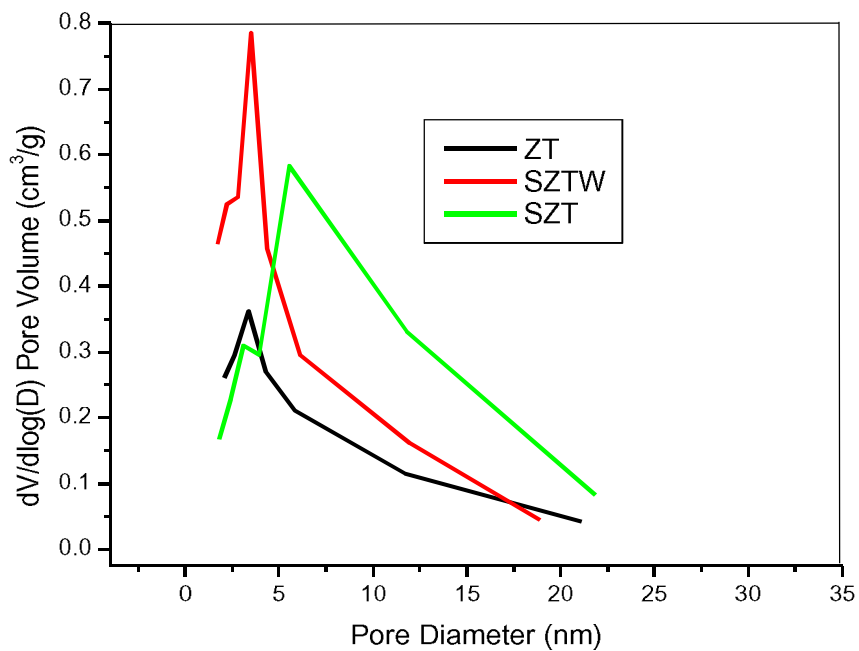
Figure 4. 17 Pore size distribution of samples ZT; SZT; SZTW

Figure 4. 18 Surface area and Porosity Analyzer

4.1.5 Temperature Programed Desorption (NH₃- TPD)

Temperature-Programmed Desorption (TPD) is one of the mostly used and simple method to calculate the acidic sites on oxide surfaces. There are three kinds of molecular analyses usually used for characterizing acidic sites using TPD:

Ammonia. 2) Non-reactive vapors. 3) Reactive vapors.

In this research work, ammonia TPD is used for acidity measurement [Oliveira et al., 2015]. Due to the simplicity, ammonia TPD is a widely used technique for the characterization of acid site densities in solid acids materials. Offen ammonia overestimates the quantity of acid sites. The smaller molecule size permits ammonia to

enter into all pores of the solid materials whereas larger molecules, commonly found in cracking and hydrocracking reactions, only have access to large micropores and mesopores. Ammonia is a very basic molecule, which is proficient of titrating weak acid sites that may not participate in the activity of catalyst.

The profile of temperature-programmed desorption of ammonia (NH_3-TPD) over the catalysts was carried out in a U type quartz reactor (ID = 6 mm) packed with about 0.1 g of catalyst using TPD/TPR Instrument [Micromeritics Chemisorb 2750, Fig. 4.22]. The samples were pre-treated for two hours at 150°C, under argon flow of 20 ml min^{-1}, followed by cooling to room temperature in order to remove any physisorbed impurity on the surface of the sample. After pre-treatment, the samples were subjected to chemisorption step using ammonia in helium (9.8%, mol/mol) at flow rate of 20 ml min^{-1} at room temperature, for 30 minutes. Thereafter, the system was purged with helium at room temperature for two hours. In order to remove extra ammonia molecules, the material was treated for 30 minutes at 120°C under helium flow (20ml min^{-1}). This step was followed by thermal programmed desorption analysis, in which the sample was heated from 100 to 600°C, at a rate of 10°C min^{-1} under helium flow (20 ml min^{-1}). The amount of desorbed ammonia was detected with thermal conductivity detector.

Concentration and acid sites strength evaluated by NH_3-TPD (i.e. expressed as an amount of NH_3 desorbed per gram of catalyst) is presented in Table 1. The TPD profile of pure oxides are shown in Fig.19. All the sample show low acidity as shown profile the intensity of peak low as compared to sulphated and TPA impregnated samples. The

NH$_3$-TPD profiles of the SZT and SZTW catalysts are shown in Fig.4.20. Two fundamental characteristics can be identified: i.e. (i) the intensity of peaks at which maximum desorption occurs and (ii) the temperature at which such peaks occur. The intensity is related to the amount of acid sites [Miyamoto et al., 2008]. Also, the highest temperature at which the point of maximum desorption occurs, the acid strength was greatest [Camiloti et al., 1999; Miyamoto et al., 2009]. Obtained results demonstrate the presence of acid sites of different strengths in these solids. The desorption peaks of TPD profiles located at 100–200°C, 200–400°C and 400-600°C can be assigned to weak, moderate and strong acid sites respectively [Wang et al., 2013, Kumar et al., 2015]. The peak above high temperature are due to the decomposing of ammonia molecules.
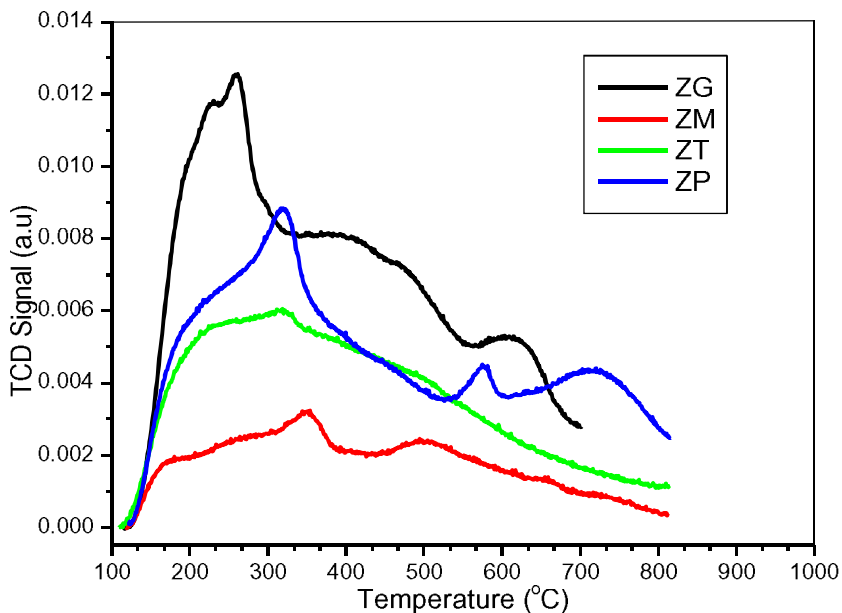

Figure 4. 19 TPD Profile of samples ZT; ZT; ZP; ZG
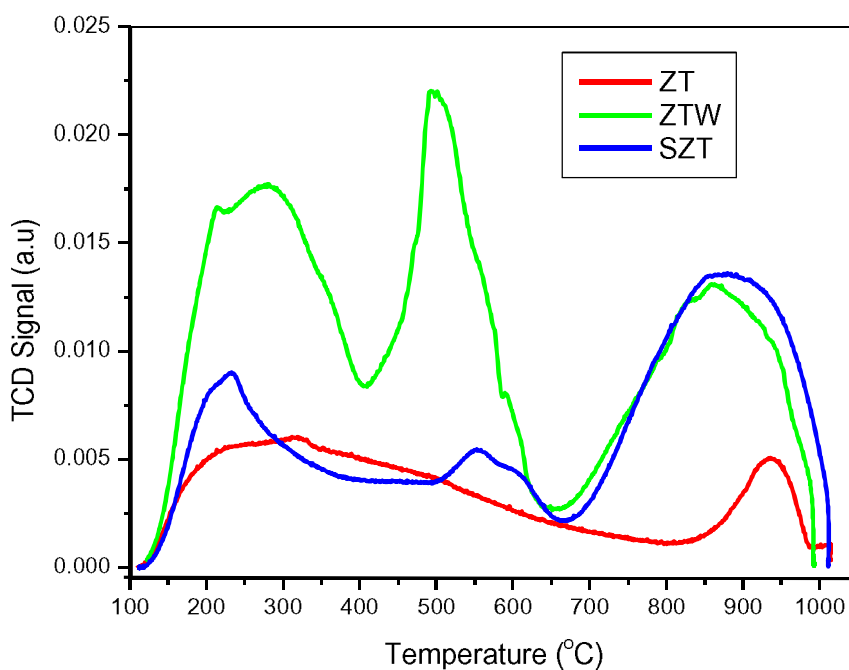
Figure 4. 20 TPD Profile of samples ZT; SZT; SZTW

4.1.6 Temperature Programed Reduction (H_2 – TPR)

Temperature programmed reduction (TPR) is a broadly used technique for the characterization of mixed metal oxides and metal oxides dispersed on a support. This technique provides quantifiable information of the reducibility of the oxides surface and about reducible surface heterogeneity. In this technique, a reducing gas mixture (3-17% hydrogen diluted in nitrogen or argon) flows over the solid materials. A thermal conductivity detector (TCD) is used to observe the changes in the thermal conductivity of the gas stream. TCD signal obtained between concentration vs time and temperature represent the total volume of gas for reduction. The redox properties of all the synthesized samples were determined by TPR profile using temperature program

desorption/ temperature program reduction (TPD/TPR), [Micromeritics, 2750 instrument] with 10% hydrogen diluted in argon (30 mL min^{-1}). Fig. 4.21 depicts the TPR profiles of ZT, SZT and SZTW materials, maximum peak indicates the temperature corresponding to the maximum reduction rate.

H_2-TPR technique provides valuable information about the reducibility of individual species, making it a useful tool to study heteropoly acid based catalytic materials. The thermal reduction behavior of pure zirconia sulphated zirconia and TPA loaded zirconia catalysts is shown in Fig. 4.21. Vera et al. (2002) suggested that the peak at temperature of 500-600°C is attributed to a surface process of lattice oxygen elimination (formation of anionic vacancies) and the reduction of Zr^{4+} to Zr^{3+} in the surface of zirconia sulfate during hydrogenation process. During these processes, it also releases sulphate from the surface of sulphated zirconia. Therefore, it can be concluded that all TPR peaks at low and high reduction temperatures are related with desorption of sulfate species.

The TPR of pure zirconia showed small hump for H_2 uptake at around 557°C [Hoang et al., 2000]. However, in sulphated zirconia, a sharp peak was obtained at 576°C due to the reduction of sulphate ion, which also has a trend to increase with increase in concentration of sulphuric acid during the preparation of sulphated zirconia [Aristizabal et al., 2008]. In SZTW, strong reduction peak appeared at the temperature higher than the decomposition of TPA. It begin to decompose at 450°C losing 1.5 H_2O and its thermal decomposition was completed above 610°C [Rao et al., 2008; Kozhevnikov et al., 2007]. There is a broad weak TPR peak in the region 400–550°C, assigned to the deprotonation of acid with concurrent non-reductive loss of lattice

oxygen [Rao et al., 2008; Chimienti et al., 2001]. The reduction region at 550-775°C in TPA loaded zirconia, is generally due to the extensive reduction of its kegging ion, which is observed to be shifted toward the upper range with increasing loading of TPA [Rao et al., 2008; Kozhevnikov et al., 2007]. The shifting of maximum peak to higher temperatures is shown in Fig.4.21, which suggests that the dispersed TPA decomposition on zirconia support increase reduction temperature due to TPA. The reduction above 750°C is due to the reduction of decomposition product WO_3.
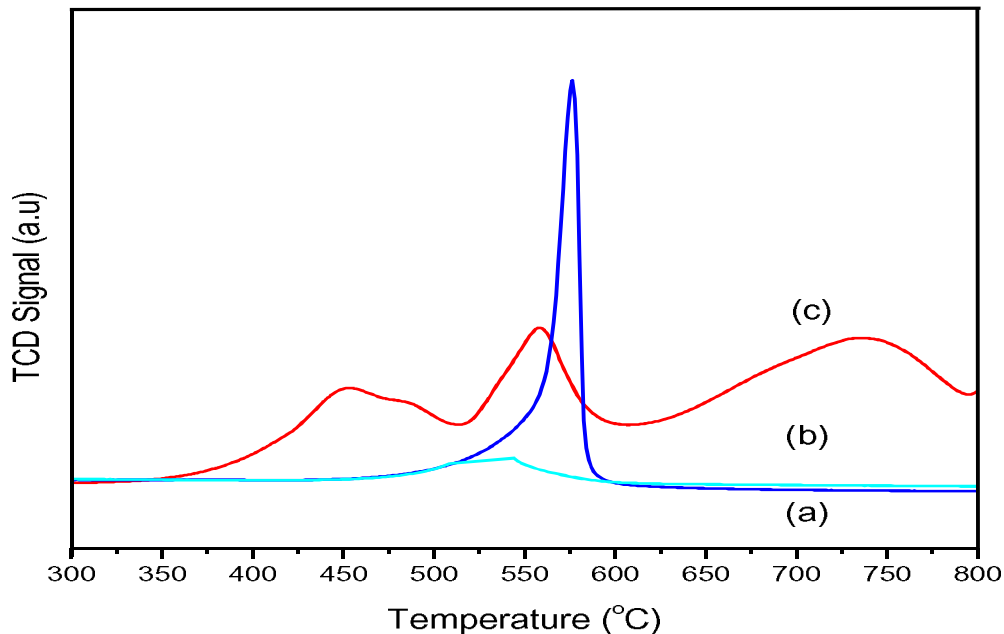

Figure 4. 21 TPR profile of samples (a) ZT (b) SZT (c) SZTW
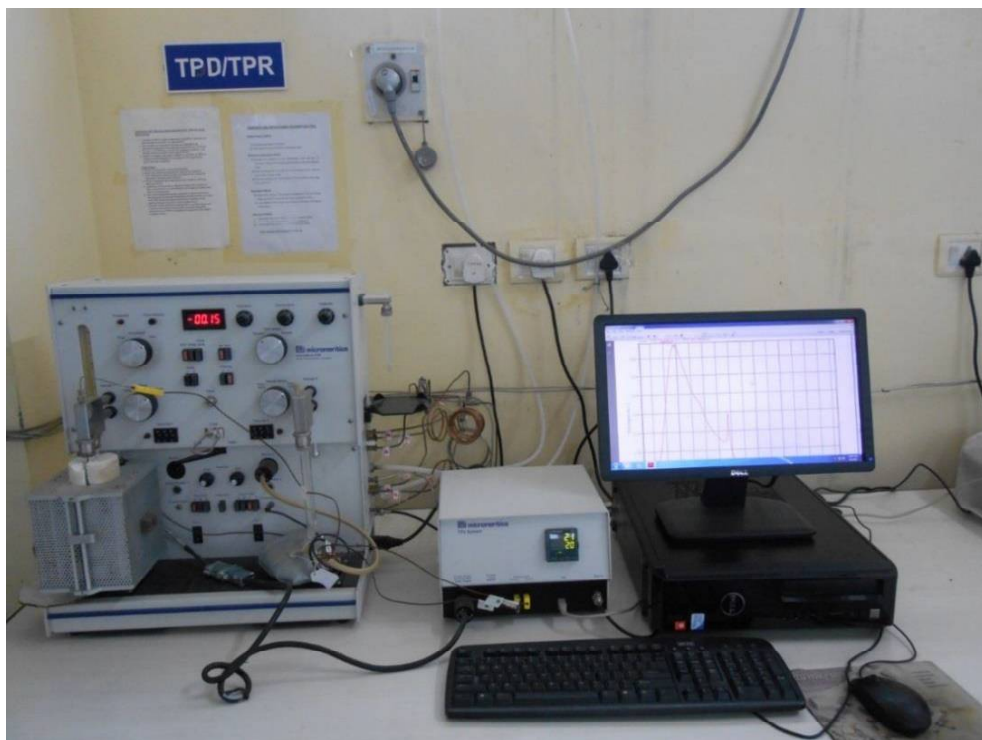
Figure 4. 22 TPD/TPR instrument

4.1.7 Thermogravimetric Analysis (TGA)

Thermogravimetric analysis or thermal gravimetric analysis (TGA) is an important technique for thermal analysis of solid materials, changes in physical and chemical properties are determined by increasing temperature (with constant heating rate), as a function of time (with constant temperature or constant weight loss) [Coats et al., 1963]. It provides information about physical phenomenon, such as sublimation, vaporization, absorption, desorption and others [Coats et al., 1963]. Generally, it is used to measure selected characteristics of materials that exhibit either weight loss or gain due to oxidation, decomposition, or loss of volatiles.

The TGA profile was carried out using TG-DTA instrument [SDT Q600 V8.3101] with temperature ranging from room temperature to 900°C. The sample was placed in

platinum crucible and analyzed under nitrogen flow with heating rate of 10°C min^{-1}.
Pure zirconia showed three stage of weight loss, between 25°C to 800°C shown
in Fig.4.23. First weight loss between 25°C to 110°C was attributed to the removal of
water molecules of the surface; the second mass loss, approximately between 290°C t
o 450°C was due to dehydroxylation of zirconyl hydroxide. Third stage between
450°C to 800°C, weight loss was attributed to the dehydration of hydrated zirconium
oxide. The trend of loss of water suggested the transformation of zirconium hydroxide
to zirconia [Sato, 2002; Srinivasana et al., 1991]. In case of sulphated zirconia, five
weight loss steps were obtained (Fig 5.23); the first step between 25°C to 110°C was
assigned to the removal of physically adsorbed water, whereas the other three stages,
between 250°C to 520°C attributed to dehydration process. The mass loss at higher
temperature, between 670°C to 730°C was assigned to the decomposition of sulphate
group [Khalaf, 2009, Reddy et al., 2006]. In sulphated zirconia, there is 5% weight loss
observed due to the decomposition of sulphate ion. TGA studies also suggest that the
prepared catalyst stable up to 650°C. TGA profile of tungstophosphoric acid
($H_3PW_{12}O_{40}$) is shown in Fig. 4.24. The curve shows that the significant changes in
weight loss of this compound are found in the range of ambient to 300°C. The TGA
profile shows an endothermal signal around 68°C and 190°C, due to the removal of
physisorbed and structural water present in the HPAs. The exothermal signal around
612°C is characteristic of this compound and represent the decomposition of its Keggin
type structure in tungsten oxide and tungsten-phosphorus [Ivanov et al., 2004; Manuel
et al., 2014] with no weight loss. The TGA profile of pure TPA shows high weight loss
compared to zirconia materials as clear from the Fig. 4.24 [Zimmermann et al., 2002].
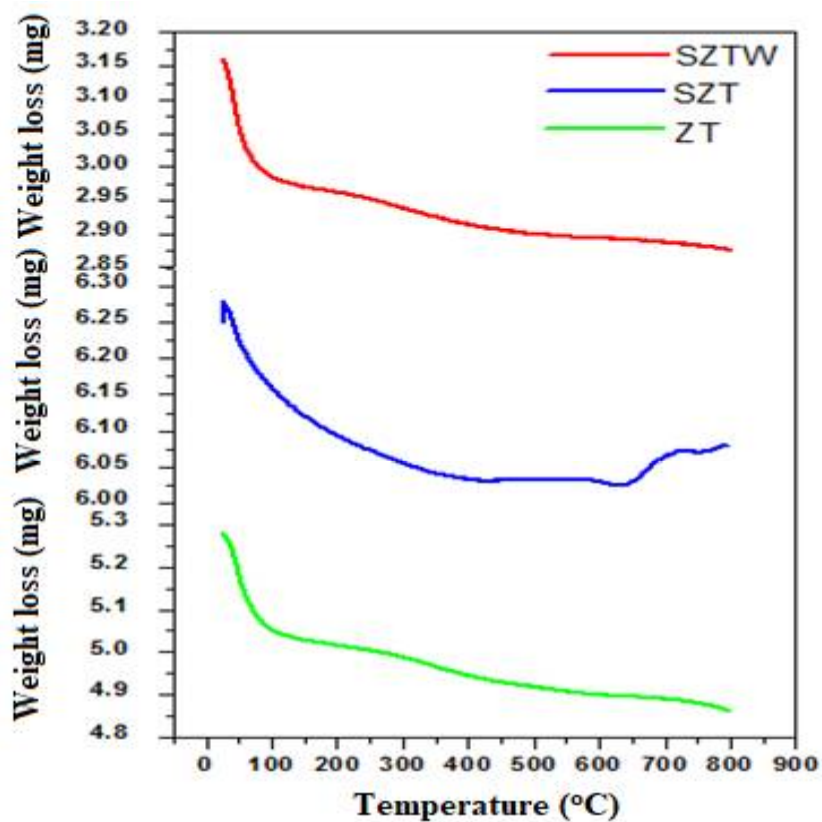
Figure 4. 23 TGA Curves of Samples ZT; SZP; SZTW
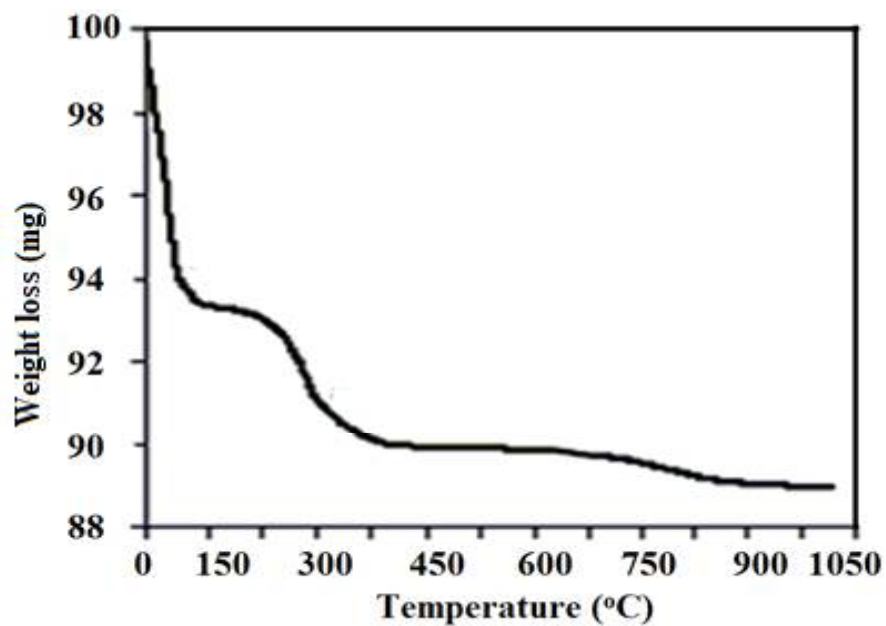
Figure 4. 24 TGA Curves of TPA

Table 4.1 Physico - chemical properties of hydrothermal synthesized samples (ZT)

Sample	S_A (m²/g)	V_P (cc/g)	D_P (nm)	S_P (nm)	A_T (ml/g)	D_B (g/cc)	Crystallinity
ZT	245	0.50	7.59	24.80	0.111	0.53	Crystalline
SZT	288	0.47	8.51	20.95	0.330	0.57	Crystalline
SZTW10	240	0.43	6.93	25.50	0.459	0.67	Crystalline
SZTW20	225	0.37	7.89	27.05	0.513	0.76	Crystalline
SZTW30	212	0.32	6.62	28.50	0.566	0.85	Crystalline
SZTW40	200	0.25	5.58	30.10	0.616	0.93	Crystalline
SZTW50	188	0.23	4.76	31.50	0.660	1.00	Crystalline
SZTW55	175	0.21	4.05	32.40	0.672	1.05	Crystalline
SZTW60	165	0.19	3.50	33.50	0.723	1.10	Crystalline

S_A: Surface area, V_P: Pore volume, D_P: Average pore diameter, S_P: Average particle size, A_T: Total acidity

Table 4.2 Physico - chemical properties of microwave synthesized samples (ZM)

Sample	S_A (m²/g)	V_P (cc/g)	D_P (nm)	S_P (nm)	A_T (ml/g)	D_B (cc/g)	Crystallinity
ZM	135	0.29	6.60	44.60	0.091	0.59	Crystalline
SZM	175	0.27	7.07	39.92	0.317	0.62	Crystalline
SZMW10	140	0.22	6.65	43.50	0.494	0.70	Crystalline
SZMW20	127	0.18	5.50	44.60	0.540	0.79	Crystalline
SZMW30	117	0.15	4.19	46.45	0.578	0.84	Crystalline
SZMW40	110	0.11	3.50	48.55	0.626	0.91	Crystalline
SZMW50	95	0.09	3.25	50.60	0.672	0.99	Crystalline
SZMW55	88	0.07	2.50	51.30	0.691	1.08	Crystalline
SZMW60	80	0.05	2.00	52.20	0.718	1.18	Crystalline

S_A: Surface area, V_P: Pore volume, D_P: Average pore diameter, S_P: Average particle size, A_T: Total acidity

108

**Table 4.3 Physico - chemical properties of sample synthesized by
precipitation method (ZP)**

Sample	S_A (m²/g)	V_P (cc/g)	D_P (nm)	S_P (nm)	A_T (ml/g)	D_B (g/cc)	Crystallinity
ZP	224	0.41	6.32	26.73	0.111	0.56	Crystalline
SZP	268	0.39	7.85	22.47	0.334	0.60	Crystalline
SZPW10	230	0.32	6.25	25.80	0.380	0.67	Crystalline
SZPW20	215	0.28	5.40	28.50	0.440	0.75	Crystalline
SZPW30	201	0.23	4.60	30.42	0.495	0.82	Crystalline
SZPW40	190	0.20	3.80	32.55	0.550	0.89	Crystalline
SZPW50	175	0.17	3.30	34.60	0.620	0.98	Crystalline
SZPW55	164	0.15	2.70	35.40	0.650	1.06	Crystalline
SZPW60	156	0.13	2.10	36.52	0.674	1.12	Crystalline

S_A: Surface area, V_P: Pore volume, D_P: Average pore diameter, S_P: Average particle size, A_T: Total acidity

Table 4.4 Physico - chemical properties of samples synthesized by sol-gel Process (ZG)

Sample	S_A (m²/g)	V_P (cc/g)	D_P (nm)	S_P (nm)	A_T (ml/g)	D_B (g/cc)	Crystallinity
ZG	150	0.31	6.83	40.25	0.120	0.54	Crystalline
SZG	195	0.29	7.50	35.20	0.312	0.59	Crystalline
SZGW10	150	0.25	6.73	40.20	0.380	0.68	Crystalline
SZGW20	140	0.21	5.93	41.50	0.440	0.74	Crystalline
SZGW30	138	0.17	5.33	42.20	0.480	0.79	Crystalline
SZGW40	126	0.13	4.63	43.25	0.530	0.85	Crystalline
SZGW50	115	0.10	3.50	44.50	0.580	0.91	Crystalline
SZGW55	102	0.08	3.00	46.50	0.650	1.01	Crystalline
SZGW60	93	0.06	2.50	48.25	0.690	1.10	Crystalline

S_A: Surface area, V_P: Pore volume, D_P: Average pore diameter, S_P: Average particle size, A_T: Total acidity

In this chapter, the prepared samples characterized viz. SEM analysis FTIR, TPD, TPR, and TGA, and found that the catalyst prepared by hydrothermal synthesis showed high surface area and acidity. The catalytic activity of catalyst, performance and evaluation is discussed in chapter V.